JOURNAL OF MATERIALS SCIENCE 27 (1992) 4647–4650

Structural properties of ZnS_xSe_{1-x} thin films on GaAs (1 1 0) substrate

G. N. CHAUDHARI, S. N. SARDESAI, S. D. SATHAYE, V. J. RAO*
Physical and Structural Chemistry Division, National Chemical Laboratory, Pune 411 008, India

Deposition and structural characterization of lattice-matched ZnS_xSe_{1-x} ($x = 0.056$) films on GaAs (1 1 0) and glass substrates by a new chemical growth technique have been investigated by transmission electron microscopy and X-ray diffraction, including low-angle X-ray diffraction, at different temperatures. Electron diffraction examination has revealed that ZnS_xSe_{1-x} films exhibit an amorphous nature when deposited at room temperature, and at 90 °C the films are polycrystalline with a large grain size. X-ray diffraction and morphology showed that the growth of the crystallite size increased with increasing solvent temperature. The chemical data from X-ray fluorescence confirm the enhancement of sulphur content at the interface and also establish the composition.

1. Introduction

The mixed crystals ZnS_xSe_{1-x} ($0 < x < 1$) are semiconductors with direct band gap energies ranging from 3.7–2.7 eV at room temperature (RT) at any composition [1] and are very attractive for many device applications [2–7] for which high-quality epitaxial layers of the materials are required. The performance and degradation of devices depend rather critically on the lattice match between the epilayers and the substrates. ZnSe grown on GaAs provides a lattice mismatch of 0.25%. However, assuming Vegard's law [4, 8], exact lattice matching can be achieved through the incorporation of a small amount of sulphur on the selenium sublattice to give the composition $ZnS_{0.056}Se_{0.944}$. ZnS_xSe_{1-x} thin films have been grown by metalorganic vapour phase epitaxy [9, 10], molecular beam epitaxy [11, 12] and vapour transport techniques [13–15]. However, the chemical deposition method for the formation of ZnS_xSe_{1-x} ($x = 0.056$) thin films has not yet been reported.

Here we describe the growth of lattice-matched ZnS_xSe_{1-x}/GaAs heterostructures by a new chemical method and their characterization by transmission electron microscopy (TEM), X-ray diffraction (XRD) and small-angle X-ray diffraction (SAXD) measurements.

2. Experimental procedure

The ZnS_xSe_{1-x} thin film was deposited by chemical growth technique using thiourea and sodium selenosulphate solution as sulphur and selenium sources. Aqueous solution of 0.175 M zinc nitrate, 0.57 M NaOH, 0.4 M sodium selenosulphate [16] and 1 M thiourea were used to prepare ZnS_xSe_{1-x} films. Zinc nitrate solution, 5 ml, was mixed with 25 ml NaOH with constant stirring and then diluted with about 65 ml water. This solution was used as the stock solution: 5 ml stock solution were mixed with 0.7 ml thiourea and 5 ml sodium selenosulphate with constant stirring until a clear homogeneous solution was obtained. The solution was transferred to a beaker containing well-cleaned glass and GaAs (1 1 0) substrates. The GaAs (1 1 0) wafer was first etched in $H_2SO_4 : H_2O_2 : H_2O$ (4 : 1 : 1) for 30 s, then rinsed with deionized water. Films of different thicknesses were obtained by keeping the substrates in the solution for different times at different temperatures and also by repeating the deposition procedure.

The structural properties were determined by XRD (Philips PW 1730, Holland), TEM (Jeol 1200 EX, Tokyo, Japan) and the composition of these films were estimated by X-ray fluorescence (XRF) (Rigaku 3070). The deposited film was also characterized by SAXD measurements performed on a Rigaku, Japan (Model No. Rotaflex RV 200B) using CuK_α radiation. In the SAXD measurements, Seeman–Bohlin geometry was employed and the grazing angle of incidence, α, was kept at 0.5°, 0.7° and 1°. The choice of these values of grazing angle were based on the X-ray penetration in the sample. The morphology of these films was studied using TEM.

3. Results and discussion

The XRD pattern of a layer of ZnS_xSe_{1-x} grown at 90 °C is shown in Fig. 1. The net areas under the main peaks were measured in addition to the usual I versus 2θ spectrum. Growth in crystallite size in the film was

*Author to whom all correspondence should be addressed.

0022–2461 © 1992 Chapman & Hall

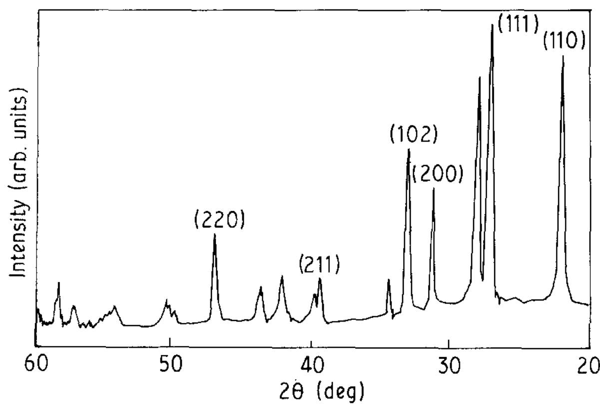

Figure 1 XRD pattern of ZnS_xSe_{1-x} ($x = 0.056$) on a glass plate.

observed when the bath temperature was increased to 90 °C, whereas the film deposited at RT was amorphous. Furthermore, the XRD intensity of the (1 1 1) plane increased with increasing bath temperature. Similar results were observed by TEM.

TEM samples were prepared as described earlier [17]. Small pieces of the sample were picked up on a holey carbon film supported over a specimen grid. Together with the samples, thin gold films were also mounted which can be used as a standard for obtaining an electron diffraction camera constant. The resolution and magnification that can be obtained with this instrument are 0.14 nm and $\times 10^6$, respectively. The equipment can be operated at 120 kV. The samples were examined in the usual bright-field imaging mode.

ZnS_xSe_{1-x} films formed at RT were agglomerates and the crystallites were not well defined; with further increase in bath temperature, say about 90 °C, the films became crystalline. Fig. 2 shows a bright-field image and SAXD pattern of the film obtained at 90 °C. The pattern consisted of spots as well as rings and due to the formation of epitaxial as well as polycrystalline ZnS_xSe_{1-x} films. When the spots of the different reflections were carefully examined, it could be seen that the innermost (1 1 1) reflections (very strong) consisted of twelve spots, much cleaner on the negative, followed by an equal number of spots on the (2 2 0) and (1 1 1) reflections. It was also seen that four reflections (spots) disposed at 90° to each other, lying on the (2 2 0) ring, were more intense as compared to the rest. This suggests that the deposits developed predominantly a 2-d (1 1 0) orientation.

The TEM morphology of the films deposited at both RT and 90 °C, was examined. The films (Fig. 3) show a granularity which enhanced the size of the flake-like grains. When the size of the particles was increased, aggregates could be seen by TEM, appearing as deposits.

The SAXD pattern of the $ZnS_{0.056}Se_{0.944}$ films deposited on GaAs at RT taken at a glancing angle of 0.5° is shown in Fig. 4a. All the diffraction lines closely match those reported for polycrystalline ZnS_xSe_{1-x}. Together with the ZnS_xSe_{1-x} phase, however, small quantities of other stoichiometric phases were also seen. Although the structural quality of this film is fairly good, it became clear that increases in the bath temperature did influence the grain growth of the film. The corresponding XRD pattern is given in Fig. 5a which clearly shows improvement in the film quality, compared to that in Fig. 4a. This condition led to the formation of a stoichiometric film at the interface. When the XRD pattern is compared with that of the films deposited on a glass plate, it is seen that the films deposited on GaAs exhibit some texture effect, possibly due to partial preferred grain orientation.

When film deposition is performed at the same bath temperature (RT) but at a higher grazing angle of incidence, the results show significant changes in film

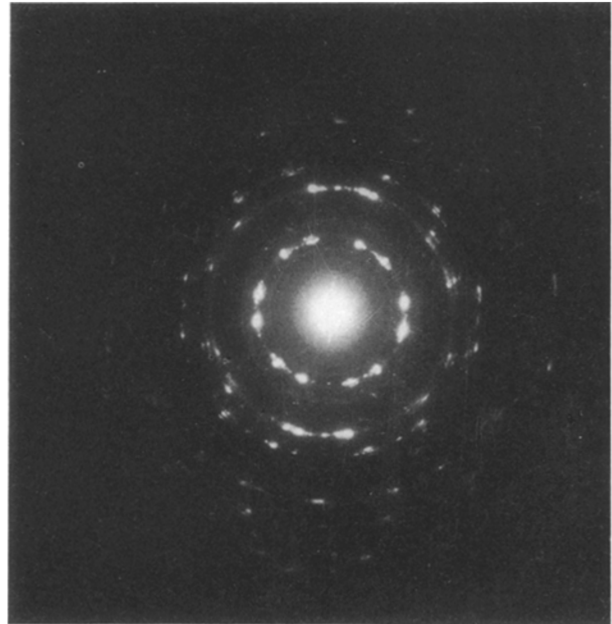

Figure 2 Electron diffraction pattern of ZnS_xSe_{1-x} ($x = 0.056$).

Figure 3 Bright-field TEM images of the ZnS_xSe_{1-x} at 90 °C.

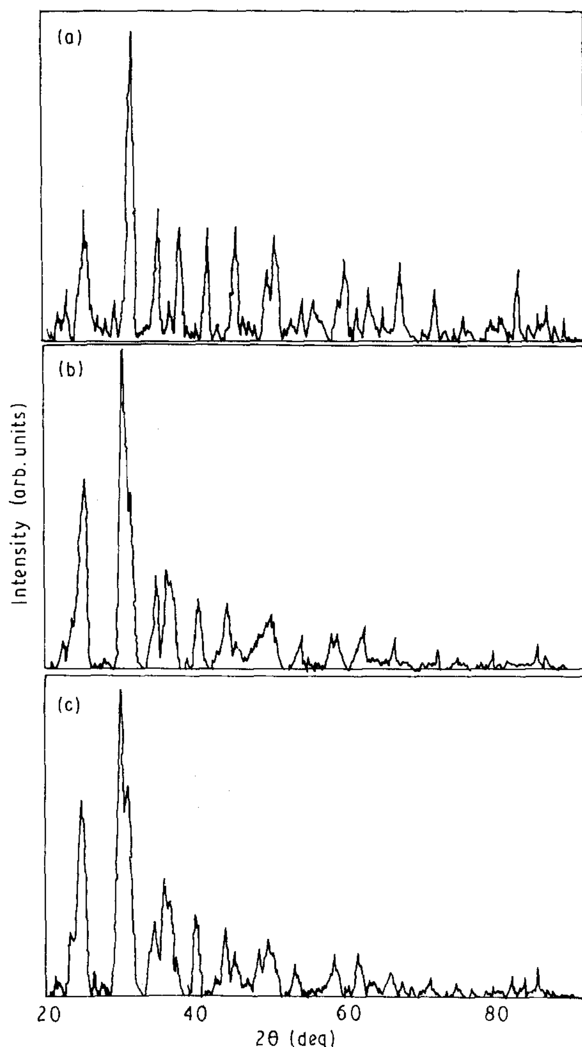

Figure 4 Low-angle XRD pattern of ZnS_xSe_{1-x} ($x = 0.056$) on *n*-GaAs (1 1 0) at different glancing angles: (a) $\alpha = 0.5°$, (b) $\alpha = 0.7°$, (c) $\alpha = 1.0°$.

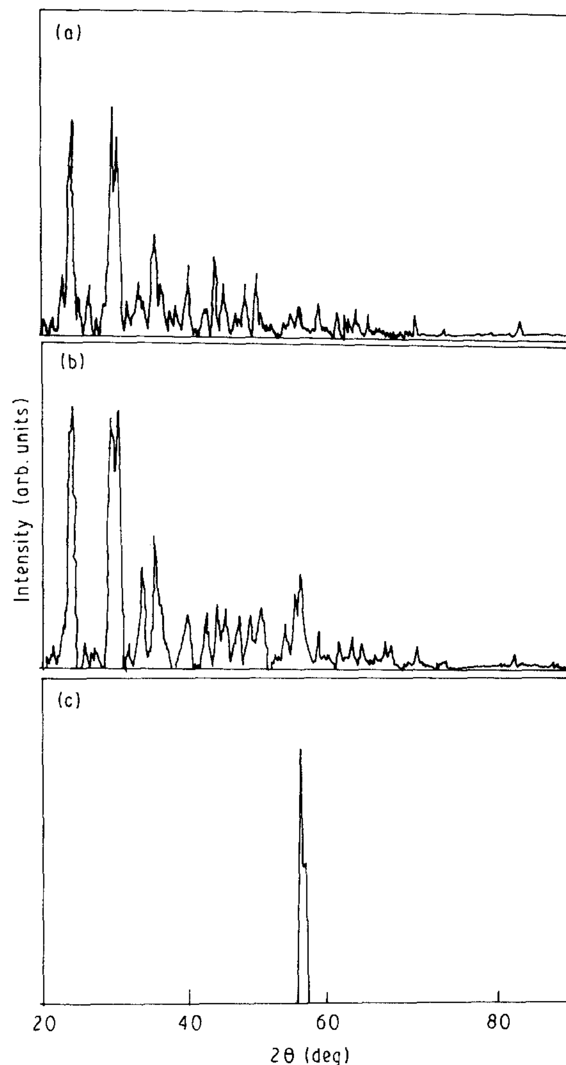

Figure 5 Low-angle XRD pattern of ZnS_xSe_{1-x} ($x = 0.056$) on *n*-GaAs (1 1 0) at different glancing angles: (a) $\alpha = 0.2°$, (b) $\alpha = 0.5°$, (c) $\alpha = 1.0°$.

properties. SAXD at an angle of 0.7° is shown in Fig. 4b; when the XRD pattern of Fig. 4b is compared with that given in Fig. 4a, it can be observed that the predominant peak at $2\theta = 24.72°$ ($d = 0.35991$ nm) is attributed to the $ZnS_{0.056}Se_{0.944}$ phase and the pattern is very weak. The same is the case with the peak at $2\theta = 29.62°$ ($d = 0.3014$ nm) which also corresponds to the same phase. Further, the broad peak structure in the region $2\theta = 44°$–$59°$ is nearly the same except in intensity. In fact, the major X-ray peaks in Fig. 4b together represent a typical pattern for the $ZnS_{0.056}Se_{0.944}$ phase, although the intensity ratios do not correspond to the bulk case, presumably due to the preferential orientation effects. The lines at $2\theta = 33.36°$ and 47.58° are presumably due to the presence of Ga_2Se_3, and those at $2\theta = 43.34°$, 52.14° and 70.82° correspond to the presence of the Zn_3As_2 phase in the sample. This is possible because of the interfacial reactions between the GaAs surface and the ZnS_xSe_{1-x} film at higher temperature. The relative contributions of these phases, as expected, differ significantly compared to those in the case represented by Fig. 4a. It is thus clear that changes in the bath temperature can lead to changes in the nature of the phase formation process at the interface. This effect is probably controlled by the stability of intermediate phases under the conditions of temperature-dependent adsorption–desorption kinetics.

The SAXD pattern ($\alpha = 1°$) of the sample deposited at $T_{bath} = 90$ °C is shown in Fig. 5c. It is interesting to compare the pattern of Fig. 5c with that of Fig. 5b, which also corresponds to the deposition at $T_{bath} = 90$ °C. It is readily seen that the highest peaks at $2\theta = 24.22°$ ($d = 0.3672$ nm) and the doublet at $2\theta = 29.38°$ and 30.26°, and other peaks, are totally absent. In fact, the entire spectrum consists of only one peak split into two lines corresponding to the $2\theta = 54°$ and 54.68° due to (1 1 0) orientation of GaAs, because the penetration depth of the incident X-ray beam is sufficiently high at $\alpha = 1$, therefore the characteristic XRD pattern reveals only the bulk structure of the GaAs substrate.

The chemical composition of the films has been estimated by X-ray fluorescence (XRF) and confirms the enhancement in sulphur at the interfaces. The sulphur and selenium concentrations were constant throughout the film.

4. Conclusion

Good-quality films of ZnS_xSe_{1-x} ($x = 0.056$), having an exact lattice match to GaAs, can be deposited by a

chemical growth technique. It has been observed from TEM and XRD via XRF results that the films are continuous and uniform even after increasing the solvent temperature. XRD showed that the film deposited at RT is amorphous and at 90 °C films are polycrystalline. The ZnS_xSe_{1-x} films are simple cubic. An electron diffraction study of the films at higher temperature shows the presence of a polycrystalline phase together with single crystal (f c c) phase with a (1 1 1) zone axis. The surface morphology of $ZnS_{0.056}Se_{0.944}$ at 90 °C is very smooth as compared to that obtained at RT.

Finally, it is concluded that the film deposited at a higher temperature of about 90 °C are pure polycrystalline films with large grain size. The crystalline quality of the lattice-matched film is improved at a moderately high growth temperature.

Acknowledgement

The authors gratefully acknowledge the financial support for this work by Department of Electronics (DOE), New Delhi. Thanks are due to Dr S. M. Chaudhari, Department of Physics, University of Poona, for recording low-angle X-ray diffraction results.

References

1. R. K. WATTS, "Point deflects in crystal", (Wiley Interscience, New York, 1977) Ch. 9.
2. D. ETIENNE, L. SOONCKINDTH and G. BOUGHOT, *J. Electrochem. Soc.* **127** (1980) 1800.
3. N. MATSUMURA, K. ISHIKAWA, J. SARAIE and Y. YOGOGAWA, *J. Crystal Growth* **74** (1985) 41.
4. K. OKAMOTO, N. ITOCH, W. OGAWA, T. KAWABATA and S. KOIKE, *Jpn J. Appl. Phys.* **27** (1988) L756.
5. T. KANDA, I. SUEMUNE, K. YAMADA, Y. KAN and M. YAMANISHI, *J. Crystal Growth* **93** (1988) 622.
6. K. OHMORI, M. OHISHI, T. OKUDA and M. HIRAMATSU, *J. Appl. Phys.* **49** (1978) 4506.
7. T. KODA and S. SHIONOYA, *Phys. Rev.* **136A** (1964) 541.
8. R. H. Bube (ed.), "Photoconductivity of Solids", (Wiley, New York, 1960), p. 252.
9. P. J. WRIGHT and B. COCKAYNE, *J. Crystal Growth* **59** (1982) 148.
10. W. STATIUS, *J. Elect. Mater.* **10** (1981) 95.
11. F. KITAGAWA, T. MISHIMA and K. TAKAHASHI, *J. Electrochem. Soc.* **127** (1980) 937.
12. T. NIINA, T. MINATO and K. YONEDA, *Jpn J. Appl. Phys.* **21** (1982) L387.
13. D. ETIENNE, J. CHEVRIER and G. BOUGNOT, *J. Crystal Growth* **37** (1977) 147.
14. J. ZHOU, H. GOTO, N. SAWAKI and I. AKASAKI, *Phys. Status Solid (A)* **103** (1987) 619.
15. H. HOTO, J. ZHOU, N. SAWAKI and I. AKASAKI, *Jpn J. Appl. Phys.* **26** (1987) 1300.
16. P. PRAMANIK and B. BISWAS, *J. Electrochem. Soc.* **133** (1986) 350.
17. K. SAITO and M. IWAKI, *J. Appl. Phys.* **55** (1984) 4447.

Received 15 April
and accepted 5 August 1991